How can tropical Pacific ocean heat transport vary?

Wilco Hazeleger [1]
Royal Netherlands Meteorological Institute (KNMI), De Bilt, The Netherlands

Richard Seager, Mark Cane, and Naomi Naik
Lamont-Doherty Earth Observatory of Columbia University, New York

August 9, 2002

submitted to J. Phys. Oceanogr.

[1] *Corresponding author address*: W. Hazeleger, Royal Netherlands Meteorological Institute (KNMI), P.O. Box 201, 3730 AE, De Bilt, The Netherlands, email: hazelege@knmi.nl

Abstract

The response of ocean heat transport in the Pacific to atmospheric variability is studied. The meridional overturning circulation in the tropics and subtropics transports heat away from the equator. The horizontal gyre circulation transports a smaller amount of heat towards the equator in the tropics. Model experiments show a relatively small reduction in heat transport in response to El Niño-like winds, although changes in heat transport by the overturning and gyre circulation are large. However, these changes tend to compensate in response to changes in the tropical winds. That is, the overturning transport reduces and the gyres spin down. This compensation breaks down when the Indonesian Throughflow is allowed to vary. In general, during El Niño-like conditions the volume transport in the Indonesian Throughflow is small and causes a large reduction of poleward heat transport in the South Pacific. Also, changes in heat loss in the midlatitudes can significantly change the heat transport in the tropics by an enhanced buoyancy-driven overturning that reaches into the tropics. These results are related to observed changes in the overturning circulation in the Pacific in the 1990s, sea surface temperarture changes, and changes in atmospheric circulation. The results imply that the ratio of heat transport in the ocean to that in the atmosphere can change.

1 Introduction

The excess of net incoming radiation at the top of the atmosphere in the tropics and the deficit of net radiation in the extratropics requires poleward energy transport in the atmosphere and oceans to mediate the radiative imbalance. Recent estimates, based on satellite-derived top of the atmosphere radiation and atmospheric reanalysis data, show that the ocean dominates the energy transport in the tropics (Trenberth and Caron, 2001). Here we will focus on the part of the ocean heat transport that occurs in the tropical Pacific. In the Pacific the ocean heat transport peaks at 0.96 PW at 15°N. In the South Pacific poleward heat transport peaks at 0.92 PW at 10°S according to Trenberth and Caron (2001). Deep hydrographic data at low latitudes is sparse. But in combination with inverse models, ocean data also indicates a relatively strong ocean heat transport at low latitudes (Ganachaud and Wunsch 2000, 2002). Ocean heat transports estimates derived from surface flux climatologies show maxima in the tropics, but with amplitudes almost a factor of two smaller than estimates from atmospheric reanalysis data.

Although meridional heat transport is one of the most fundamental properties of the climate system, the error bars on all estimates of mean ocean heat transports are large. This may explain why temporal variability in heat transport in the coupled climate system has hardly been addressed, except for seasonal variations (e.g. Bryan 1982, Jayne and Marotzke 2001). However, climate in the tropical Pacific has undergone large variations at low frequencies (Guilderson and Schrag 1998, Zhang et al. 1997) and might also change in the near

future (Timmermann et al. 1999). It is not known how the atmosphere and ocean heat transports are involved in these climate changes.

McPhaden and Zhang (2002) showed that the volume transport by the meridional overturning in the Pacific reduced in the 1990s. They suggested that this induced a reduction of the poleward meridional heat transport and warming of sea surface temperature in the tropical Pacific in the 1990s. In the same period, satellite-derived top of the atmosphere radiation showed a reduction in the net radiative gain of the tropics (Wielicki et al. 2002). If this is true then the total ocean and atmospheric heat transport varies. However, it is unclear how the partitioning between atmospheric and oceanic heat transport changed during this period.

Bjerknes (1964) hypothesized that oceanic and atmospheric heat transport variations at low frequencies compensate for each other to retain a constant total heat transport. This requires no variability in the top of the atmosphere radiation. The observations suggest this is not the case. In contrast to Bjerknes, Held (2001) argues that the heat transport in the tropical ocean and atmosphere go hand in hand. He assumes that the Hadley Cell is the major agent of atmospheric heat transport while in the ocean the shallow wind-driven Subtropical Cell transports most heat. Since the mass transports in both cells are constrained by the same momentum flux at the air/sea interface, a constant partitioning between atmospheric and oceanic heat transport is found. In this case, a change in the Hadley Cell and Subtropical Cell will require a change in the top-of-the-atmosphere radiation for the climate to stay in equilibrium.

An idealized model of the subtropical cell which uses the observed wind stress and SST distributions (see Appendix 1, the model is essentially the same as that presented by Klinger and Marotzke (2000) and used by Held (2001)), shows a distribution of heat transport that is qualitatively similar to observations. The maximum in the heat transport is at low latitudes. However, the maximum amplitude is only 0.53 PW at 7°N (see Fig. 1). The difference between the heat transport obtained from the simple model and the estimates derived from the atmospheric reanalysis data shows that heat transport by the wind-driven overturning circulation can only partly explain the total oceanic heat transport. In this simple model the heat transport by the horizontal geostrophic flow has been neglected [2]. A crude estimate of the amplitude of the heat transport carried by the horizontal gyres shows that it is not negligible. It acts to oppose the heat transport by the Subtropical Cell. The equatorward heat transport by the gyres in the tropics is a consequence of the horizontal circulation bringing warm water towards the equator in the west and transporting relative cooler water poleward in the east. The idealized picture of heat transport by two overturning cells in the Pacific is also broken by the presence of the Indonesian Throughflow (ITF). The ITF

[2] As noted by Held (2001), a scaling argument indicates dominance of Ekman drift versus geostrophic transport near the equator, but careful analysis shows that both are of the same order and opposite (see Pedlosky 1996, page 14,15).

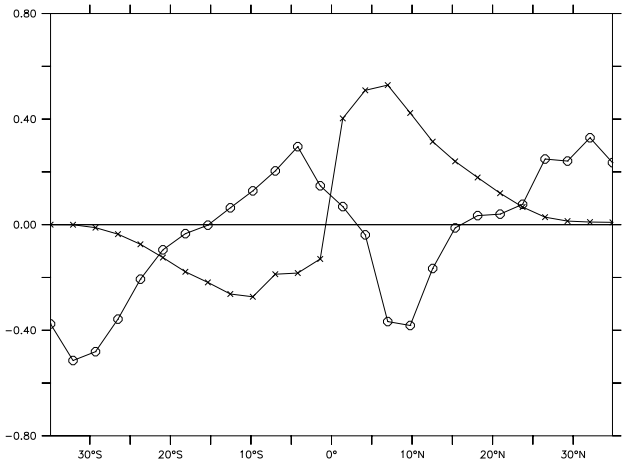

Figure 1: Heat transport estimates in the Pacific Ocean (in PW=10^{15}W) derived from the simple models outlined in the Appendix. Continuous with cross symbols: from idealized model of the wind-driven overturning using winds from the NCEP/Reanalysis data (Kalnay et al. 1997) and sea surface temperatures from the model introduced in section 2. Continuous with circles: from idealized model of gyre heat transport using NCEP/Reanalysis winds, and temperatures from the model.

transports vast amounts of heat from the Pacific into the Indian Ocean. Model simulations indicate that the ITF warms the Indian Ocean and cools the Pacific (Hirst and Godfrey 1993). Much of the heat transfered from the Pacific into the Indian Ocean is lost to the atmosphere in the Indian Ocean, especially in the Agulhas Current region (Schneider 1998). It has been observed that the ITF transport varies strongly during the ENSO cycle (Meyers 1996, Fieux et al. 1996, Vranes et al. 2002).

The failure of the idealized picture of heat transport carried by the two overturning cells in atmosphere and ocean has serious implications for how the climate varies and responds to variations in the forcing. In contrast to the picture presented by Held (2001) it may have the freedom to change the partitioning of the total heat transport between the atmosphere and ocean. This prompted us to study the ocean heat transport in a more realistic model of the Pacific. We consider the response of the ocean to variations in atmospheric forcing in order to better understand the coupling between atmospheric and oceanic heat transport. Initially we focus on El Niño-like forcing anomalies. We will determine the stationary response, so that the results are not representative of the interannual ENSO phenomena, but are instead applicable to decadal and longer term variability in the tropical Pacific (Zhang et al. 1997, McPhaden and Zhang 2002). We will also study the response of the heat transport to a change in the ITF transport. Tracer observations show that thermocline water in the tropics is of extratropical origin (e.g. Toggweiler et al. 1991). The interaction of water masses between extratropics and tropics may also impact the heat transport at low latitudes. Once

subducted in the extratropics water masses transfer to the tropics while their properties hardly change in the nearly adiabatic interior of the ocean. On decadal time scales the impact of subduction of thermal anomalies from the extratropics on tropical variability is small, but on longer time scales it has been shown that the tropics can respond to extratropical variability (Hazeleger et al. 2001a,b). Therefore, the response of tropical ocean heat transport to extratropical forcing anomalies is also studied.

The ocean model that is used is coupled to an atmospheric mixed layer model. The model computes its own surface fluxes of latent and sensible heat and longwave radiation. The model is less constrained than nature in that there is no equivalent of the globally averaged zero net radiative flux requirement at the top of the atmosphere. Nevertheless, it needs to be remembered that the tropical ocean heat transport varies mostly as a result of mechanical forcing of the ocean circulation and diapycnal mixing. The changes in mechanical forcing we apply are realistic and the changes in ocean heat transport will also be realistic unless there are major changes in solar radiation, cloud cover, or ITF heat transport. The experiments will provide an estimate of by how much, and by what mechanisms, the ocean heat transport varies during low frequency climate variations and provide suggestions for how the atmospheric heat transport or total radiation will need to adjust.

2 Experimental setup

2.1 model

The experiments are performed with a primitive equation ocean model (Visbeck et al. 1998, Seager et al. 2001, Hazeleger et al. 2001a,b). The model has a resolution of 2.5° by 2.5° in the midlatitudes. The resolution in the meridional direction increases toward 0.5° at the equator. The model has 28 levels in the vertical. The model domain spans from 62°N to 62°S and from 90°E to 70°W. In the control experiment the ITF transport is set at 10 Sv and the Bering Strait is closed. The model contains a Krauss-Turner bulk mixed layer formulation and a one and a half layer thermodynamic ice model. An isopycnal thickness mixing scheme is incorporated. The vertical mixing has a background viscosity of 10^{-4} m^2 s^{-1} and a background tracer diffusion of 10^{-5} m^2 s^{-1}. The vertical mixing depends on the Richardson number. All side boundaries are closed and temperatures and salinities are restored to observations (Levitus and Boyer 1994; Levitus et al. 1994) when the model boundaries are ocean points. Also sea surface salinity is restored to observations (Levitus et al. 1994).

The ocean model is coupled to an atmospheric mixed layer model (Seager et al. 1995) to create the so called Lamont Ocean Atmospheric mixed layer Model (LOAM). The potential temperature and the humidity in the atmospheric mixed layer are computed from a balance between advection, surface fluxes, fluxes at the top of the mixed layer, and radiative fluxes.

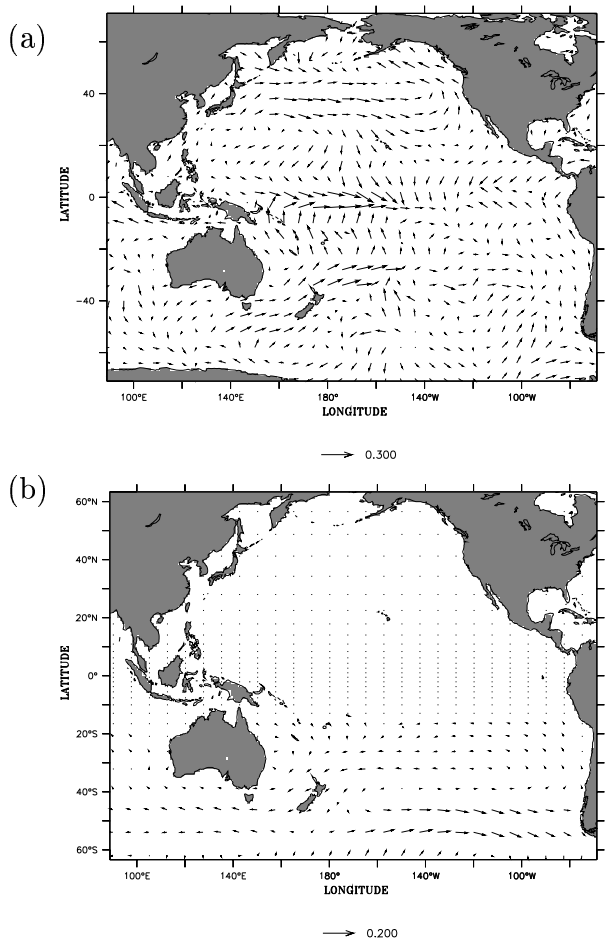

Figure 2: (a) Anomalous El Niño-like wind stress pattern (N m^{-2}) used for experiments with tropical forcing anomalies (NINO, NINO-ITF5, and same pattern with opposite sign for NINA, NINA-ITF15, see table 1). (b) Anomalous wind stress pattern used for experiments with South Pacifc forcing anomalies (SPD).

In addition cooling by storms is parameterized (Hazeleger et al. 2001a). The wind speed and the wind stress are prescribed as well as air temperature and humidity over the land points (NCEP/Reanalysis, Kalnay et al. 1996). Also the fractional cloudiness and solar radiation are prescribed (International Satellite Cloud Climatology Project, Bishop and Rossow 1991). The surface sensible and latent heat fluxes and the net surface radiation are internally computed in the model such that the SST is not overly constrained.

The model has been spun up for 80 years with the forcing as described above. The upper ocean is in equilibrium with the applied forcing. We refer to Hazeleger et al. (2001a) for more details on the model and a description of the climatology.

2.2 Experiments

We investigate the response of the ocean heat transport in the model to changes in the atmospheric forcing (see Table 1). The dominant mode of climate variability in the Pacific is the El Niño Southern Oscillation (ENSO). It is most energetic at interannual time scales, but on decadal time scales ENSO-like variability occurs as well (Zhang et al. 1997). Therefore, to study the response of ocean heat transport to atmospheric variability in the Pacific it is natural to use the atmospheric part of the ENSO pattern as anomalous forcing. We obtained this pattern by regression of the wind stress, surface winds, and wind speed on the annual surface temperature anomaly in the NINO-3 box (150°W-90°W; 5°N-5°S) (the wind stress pattern is shown in Fig. 2a, data from Da Silva et al. 1994). The wind pattern consists of a relaxing of the trade winds in an El Niño case (experiment NINO) and an increase in a La Niña case (experiment NINA).

It has been observed that the strength of the ITF varies with the phase of the ENSO cycle. During an El Niño the trade winds relax and less water is transported through the ITF. The opposite occurs during a La Niña (Meyers 1996, Fieux et al. 1996, Vranes et al. 2002). In our model, the ITF is prescribed. To study the effect of its strength, we performed an experiment with weak ITF (5 Sv) and El Niño-like wind anomalies (NINO-ITF5) and an experiment with a strong ITF (15 Sv) and La Niña-like wind anomalies (NINA-ITF15). Note that in the present model surface heat fluxes are internally computed and free to adjust, in contrast to the experiment with completely closed ITF presented by Hirst and Godfrey (1993). However, the model does not capture dynamical coupled feedbacks such as described by Schneider (1998).

In order to study sensitivity of ocean heat transport to extratropical forcing anomalies we applied an anomalous wind pattern in the midlatitudes of the Southern Hemisphere (exp. SPD1 and SPD2). This wind pattern is obtained by a regression of wind stress and wind speed on the time series of the first Emperical Orthogonal Function of annual anomalies of SST in the South Pacific (south of 20°S). The winds have been tapered to zero around 20°S. This anomalous forcing consists mainly of an increase of the westerlies to the east of the date line between 40°S and 50°S and a reduction of the westerlies to the west of the date line. The trades also enhance between 20°S and 30°S to the east of 140°W (Fig. 2b).

In the model, the anomalous forcing acts through the momentum flux at the sea surface and wind speed and direction that effect the surface heat fluxes. To address both components separately we performed one run with increasing wind stresses (exp. STRESS) and a run with increasing wind speed (exp. SPEED).

The experiments have been run for 20 years with the perpetual anomalous forcing. The tropical circulation is well adjusted within the 20 years. The adjustment to extratropical forcing takes longer and those experiments have been run for 40 years. We use data from the last year of the simulations.

Experiment	*Pattern*	*ITF transport*
Control	-	10 Sv
NINO	Fig 2a	10 Sv
NINA	Fig 2a (opposite sign)	10 Sv
NINO-ITF5	Fig 2a	5 Sv
NINA-ITF15	Fig 2a (opposite sign)	15 Sv
SPD1	Fig 2b	10 Sv
SPD2	Fig 2b (opposite sign)	10 Sv
SPEED	10 % increase wind speed with respect to Control	10 Sv
STRESS	10 % increase wind stress with respect to Control	10 Sv

Table 1: Experiments.

3 Results

3.1 Climatological ocean heat transport

Figure 3 shows the meridional ocean heat transport in the Indo-Pacific Ocean in the control experiment. The meridional heat transport is equal to:

$$OHT = \rho_w c_p \int_H^0 \int_E^W vT dx dz, \tag{1}$$

where ρ_w is the density of seawater, c_p the specific heat, v the meridional velocity, and T the potential temperature. The temperature fluxes are integrated from top (0) to bottom (H) and from east (E) to west (W) to obtain heat transports. Note that mass flux through the boundaries must be zero for the heat transport to be invariant. In some cases we will mask out the Indian Ocean. In that case the temperature will be referenced to the basin mean temperature.

To identify different physical mechanisms of meridional heat transport, the heat transport has been decomposed into three components:

$$\rho_w c_p[\overline{vT}] = \rho_w c_p[\overline{v}][\overline{T}] + \rho_w c_p[\overline{v^* T^*}] + \rho_w c_p[\overline{v'T'}]. \tag{2}$$

Here the square brackets denote the zonal and vertical integral, the $*$ denotes deviations from the zonal mean, the primes denote deviation from the time mean, and the bar denotes the time average. In general, the last term is small in our model and we will neglect it from now on. We follow the usual conventions to call the first term on the right hand side the overturning component heat transport (OHT_{ovt}) and the second term the gyre component of the heat transport (OHT_{gyre}).

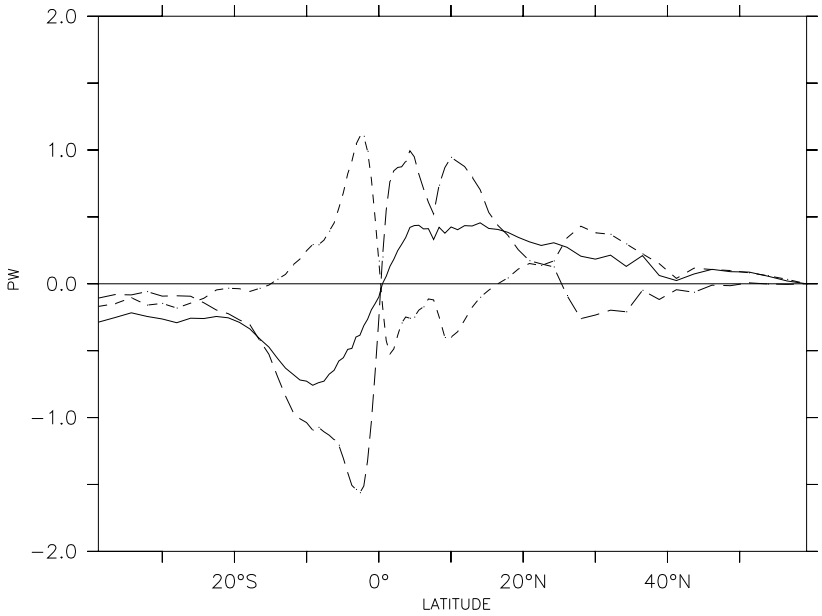

Figure 3: Heat transport in the Indo-Pacific Ocean (in PW=10^{15}W) in the Control experiment. Continuous line: total transport; long dashes: overturning heat transport (OHT_{ovt}); short dashes: gyre heat transport (OHT_{gyre}).

The total heat transport has a peak close to the equator at a value of 0.45 PW at 5°N and 0.75 PW at 9°S. These values are lower than found by Trenberth and Caron (2001), but they are within error bars of observational estimates (Ganachaud and Wunsch 2002) and they are consistent with other model simulations (e.g. Semtner and Chervin 1992).

Figure 3 also shows OHT_{ovt} and OHT_{gyre}. Especially in the tropics the individual components of the heat transport are larger than the total heat transport. The signs of both components can be easily understood from the mean circulation. The mean meridional overturning consists mainly of a subtropical cell that transports warm water at the surface away from the equator by Ekman divergence (e.g. Fig. 12a Hazeleger et al. 2001a). When the water arrives in the subtropics it has cooled and it subducts, driven by downward Ekman pumping and lateral flow through the sloping mixed layer. The subsurface adiabatic flow transfers the cooled water towards the equator where it upwells again to close the overturning circulation. This overturning is the main agent for the poleward OHT_{ovt}.

Most of the heat transport by the horizontal flow takes place in the upper thermocline. In order to understand the equatorward OHT_{gyre} in the tropics we show the deviation from the zonal velocity and temperature in the upper layer (Fig. 4a). The temperature distribution shows the warm pool in the western tropics and the cold tongue in the east stretching along the South American coast. The meridional flow is strongly poleward in the center and eastern

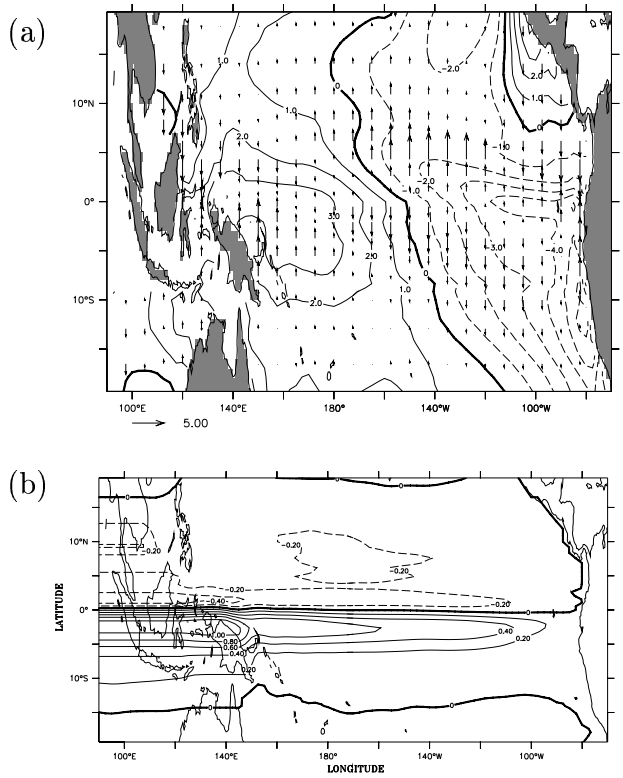

Figure 4: (a) Deviation from the zonal mean surface temperature (contours, degrees C) and surface layer meridional velocity (vectors, in 10^{-1} m s^{-1}) in experiment Control (see table 1). (b) Indefinite integral of the OHT_{gyre} (PW), that is, the vertically integrated temperature transport integrated from east to west in experiment Control. The values on the western boundary correspond to the OHT_{gyre} in Figure 3.

side of the basin caused by Ekman divergence. This flow carries water to the poles that is relatively cold compared to its zonal mean temperature, hence equatorward heat transport. When averaging the deviation of the zonally averaged meridional velocities over depth the effect of the boundary currents dominates (not shown). On the eastern side they are strongly equatorward. Since the warmest water is on the equator this also implies equatorward heat transport. This is illustrated in Figure 4b where we show the east to west indefinite integral of the gyre transport. The heat transport by the horizontal flow is equatorward over the entire zonal extension of the basin. The effect of the boundary currents on the heat transport is visible near 140°E where the integrated heat transport increases strongly towards the west.

The finding that the OHT_{gyre} is large in the tropics is not new (for instance Gordon et al. 2000 their Figure 17), but it sheds light on the question of partitioning between atmospheric and oceanic heat transport under changing forcing. The simple model of a subtropical cell accounting for almost all the heat transport is not correct for the Pacific Ocean. Consistent with the crude estimate made in section 1, the heat transport by the

horizontal gyre circulation appears to be just as important. So, the heat transports in the ocean and atmosphere need not increase and decrease together which means that the response of the partitioning to changing forcing is not a priori clear. It is with this knowledge that we are motivated to investigate the response of tropical OHT to anomalous atmospheric forcing, starting with the response to ENSO-like atmospheric forcing.

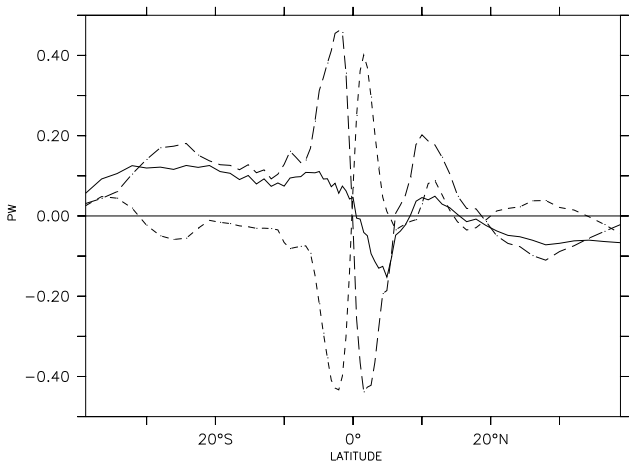

Figure 5: Difference in ocean heat transport (in PW=10^{15}W) in the Indo-Pacific between experiment NINO and experiment NINA. Continuous line: difference in total heat transport; long dashed: difference in overturning heat transport (OHT_{ovt}); short dashed: difference in gyre heat transport (OHT_{gyre}).

3.2 Heat transport during perpetual El Nino and La Nina

The SST response to El Niño-like winds (exp. NINO vs. NINA) consists of a strong warming in the central Pacific and a cooling in the western and eastern tropical Pacific and a cooling at midlatitudes (see Fig. 6a). This so called "horse shoe" pattern is roughly equivalent to the observed SST changes on time scales longer than the period of the interannual El Niño (Zhang et al. 1997), but the cooling in the eastern and western tropics do not match well with observations. The SST anomalies in the model are a stationary response to changing winds. The response differs from the transient response which is characterized by a strong warming in the cold tongue in the case of an El Niño. In the steady response the exact distribution of the anomalies in the tropics appears to be determined by the local response to wind anomalies. The wind anomalies in the Da Silva (1994) data set have relatively large amplitude in the center of the basin and they are easterly in the far eastern tropical Pacific.

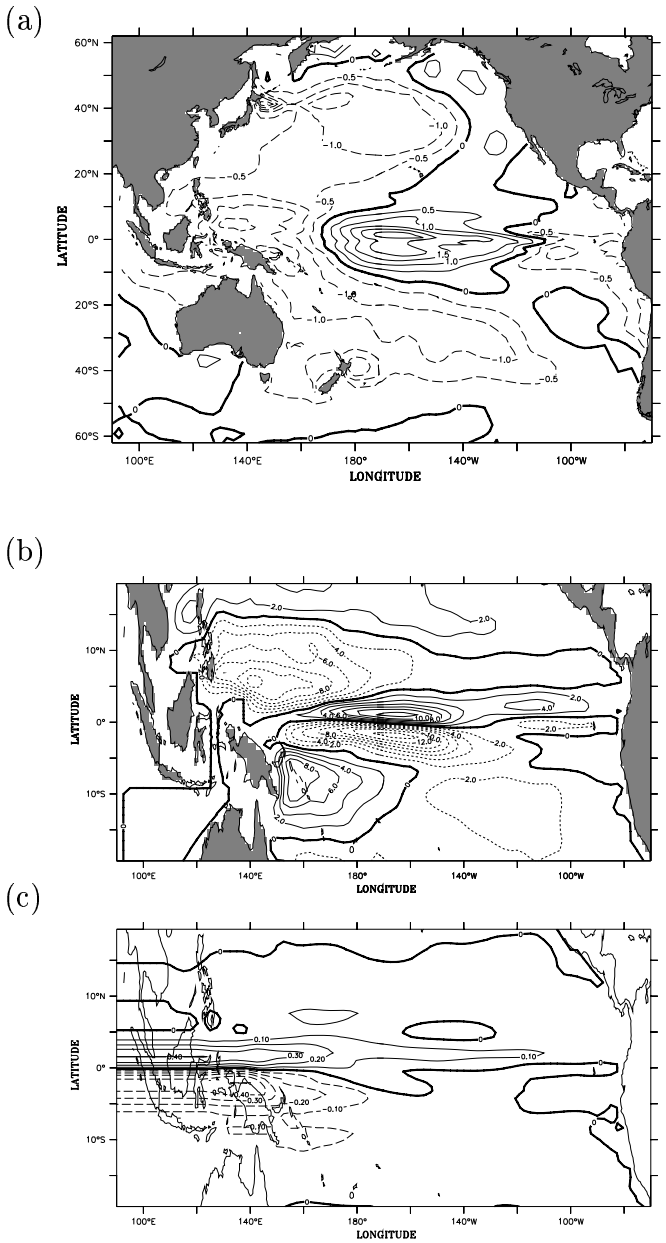

Figure 6: (a) Difference between SST (degrees C) in experiment NINO and NINA, (b) difference between barotropic stream function (Sv) in experiment NINO and NINA, (c) difference between indefinite integral of OHT_{gyre} experiment NINO and NINA.

The differences between OHT in experiment NINO and NINA are shown in Figure 5. As can be expected, large changes in the circulation occur as reflected in changes in OHT_{ovt} and OHT_{gyre}. But, strikingly, the changes nearly compensate to give a relatively small effect in the total heat transport. The heat transport is reduced by about 0.1 PW in the NINO case compared to the NINA case. This is still 20% of the total heat transport with changes in OHT_{ovt} slightly exceeding changes in OHT_{gyre}. The strength of the cancellation of OHT_{gyre} and OHT_{ovt} may be fortuitous, but the sign of the opposing effect is robust and can be explained from the response of the wind-driven circulation to the anomalous winds. The meridional mean overturning circulation is weakened in the NINO case and enhanced in the NINA case. This is a direct response to the change in the zonal wind stress. In the

NINO case reduced wind on the equator reduces the Ekman divergence and the associated upwelling. As a consequence the poleward heat transport by OHT_{ovt} is reduced by 0.4 PW compared to the NINA case.

The change in the horizontal circulation is visualized by the change in the barotropic stream function (Fig. 6b). Consistent with a reduction in the wind stress curl, the equatorial gyres spin down in the NINO experiment. The response is especially strong in the center of the basin where the largest wind anomalies occur. The change in the Sverdrup interior must be balanced by changes in the western boundary currents. Here the strongest changes in OHT_{gyre} occur (Fig. 6c). In the NINO case the western boundary current transports strongly reduce and less heat is transported towards the equator. The changes in OHT_{gyre} in the interior are small. A more detailed analysis (not shown) revealed that transport variations contribute most to the changes in the heat transport; changes in the zonal asymetry of temperature are less important.

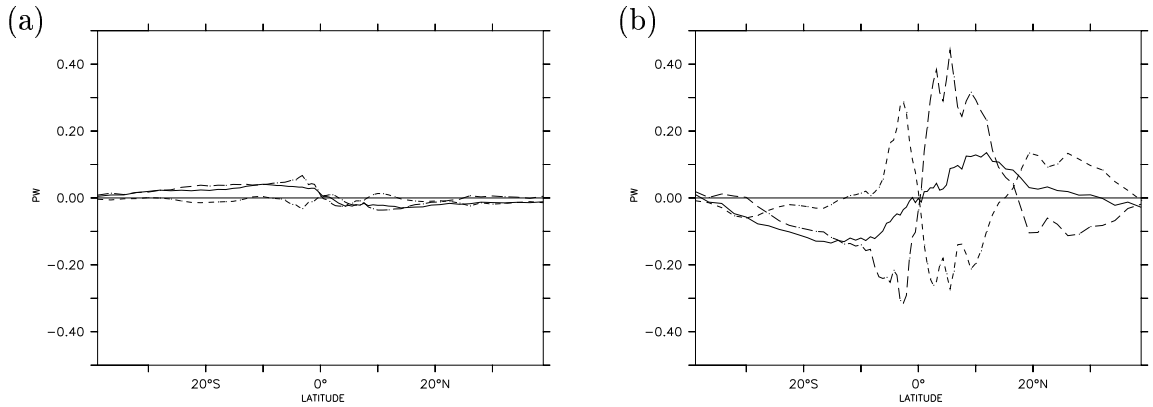

Figure 7: Heat transports: (a) Difference between run with enhanced wind speed and control run (SPEED minus Control), (b) difference between run with enhanced wind stress and control run (STRESS minus Control). Continuous line: total transport; long dashed: overturning heat transport (OHT_{ovt}); short dashed: gyre heat transport (OHT_{gyre}).

As both the strength of the gyre circulation and of the overturning circulation depend mainly on the zonal wind stress, a certain degree of compensation will always take place in response to changing zonal winds. The degree of cancellation will depend on the exact position of the upper ocean temperature anomalies and the mixing in the ocean. To demonstrate that the response is dominated by the response to changes in wind stress, we show the anomalous heat transports in an experiment where only the wind speed has been increased by 10 % over the entire basin (which effects the surface heat fluxes but leaves the circulation almost unchanged) and an experiment where the wind stress has been increased by 10 % over the entire basin (which increases the ocean circulation while the surface fluxes simply respond) (see Fig. 7). The change in the wind speed does not result in an increase of the OHT. It produces a zonally and vertically uniform temperature change which does not affect

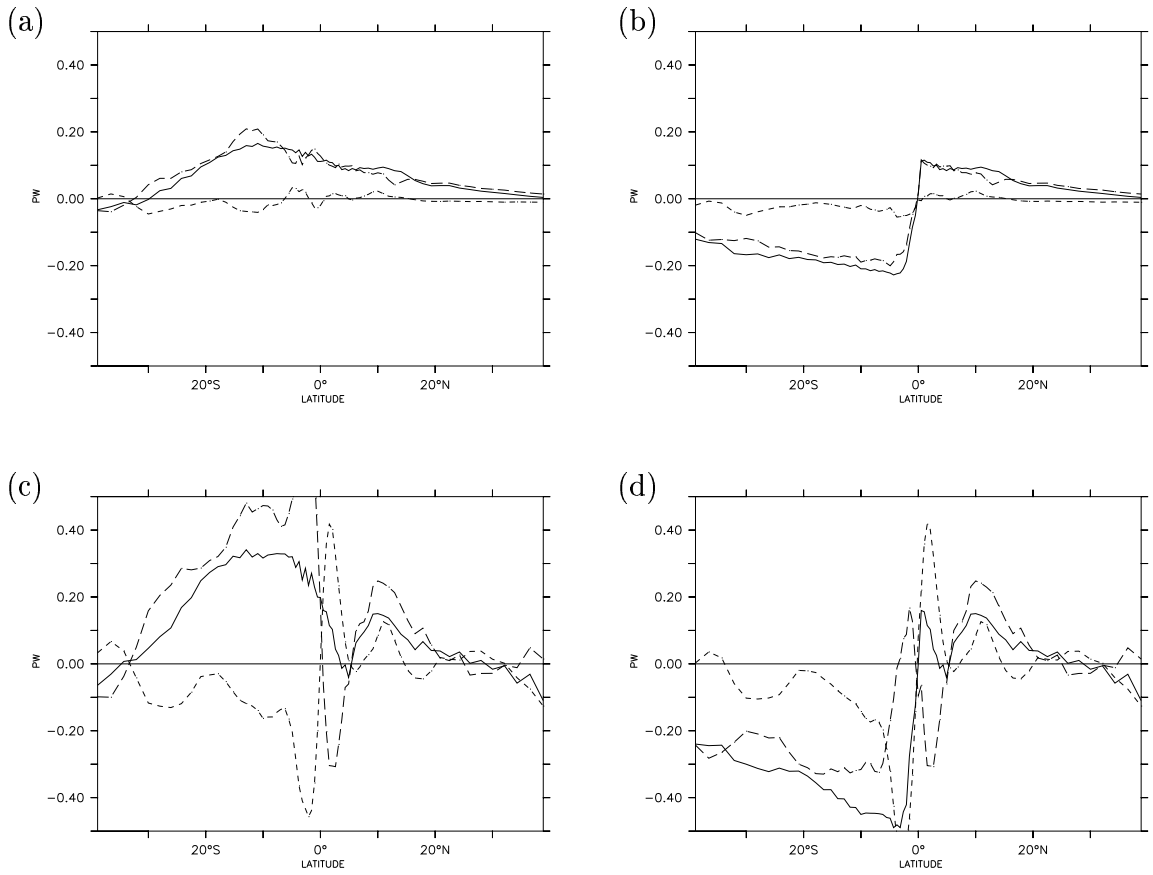

Figure 8: Heat transports: (a) Difference between ITF 10 Sv and ITF 15 Sv (NINA minus NINA-ITF15), (b) as (a) without Indian Ocean (NINA minus NINA-ITF15), (c) difference between ITF 5 Sv and El Niño winds and ITF 15 Sv and La Niña winds (NINO-ITF5 minus NINA-ITF15), (d) as (c) without Indian Ocean. Continuous line: total transport; long dashed: overturning heat transport (OHT_{ovt}); short dashed: gyre heat transport (OHT_{gyre}).

the heat transports. Changes in the wind stress, however, do change the heat transports. Heat transports by both the OHT_{ovt} and OHT_{gyre} increase as the gyres and the meridional mean overturning strengthen. The cancellation is strong but, as in the NINO and NINA cases, changes in the OHT_{ovt} exceed those in OHT_{gyre}, so the total heat transport increases by 0.1 PW for a 10 % increase in wind stress.

3.3 Impact of varying ITF on the heat transport

As mentioned before, a change in the zonal winds in the tropics affects the volume transport through the ITF from the Pacific towards the Indian Ocean. When the trade winds relax the volume transport reduces. Two experiments are performed to study the effect of varying ITF volume transport on the heat transport in the Pacific. In the first case we applied the El Niño-like anomalous winds and fixed the volume transport in the ITF to 5 Sv, instead of 10 Sv. In the second case we applied winds of the opposite sign and increased the ITF to 15 Sv.

The differences between heat transports in experiments with an ITF of 10 Sv (NINA)

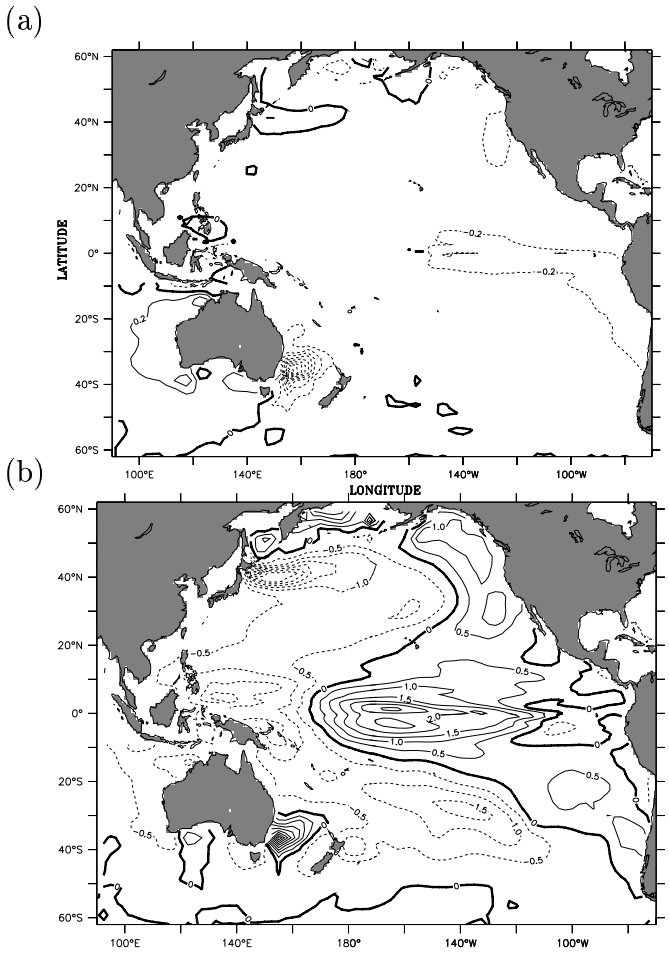

Figure 9: (a) Difference between SST (degrees C) in experiment NINA-ITF15 and experiment NINA, i.e. the effect of enhanced ITF transport on SST. (b) Differences between SST (degrees C) in experiment NINO-ITF5 and NINA-ITF15, i.e. the difference at extremes of the ENSO cycle, including variations in the ITF.

and an ITF of 15 Sv (NINA-ITF15) are shown in Fig. 8a and b. The heat transports in the Southern Hemisphere respond most strongly to the change in ITF transport, with stronger poleward heat transport when the ITF volume transport is larger. More warm water is transported from the tropical Pacific Ocean into the Indian Ocean which warms (see Fig. 9a). The South Pacific cools, especially in the East Australia Current, but also in the cold tongue in the tropics. In the Pacific alone, increased ITF causes increased northward heat transport in the Southern Hemisphere, while the divergence of the ocean heat transport, as determined by the difference in heat transport in the ITF and at 30°S causes the Pacific basin to cool when the ITF is stronger (see table 2).

This response is consistent with the complete closing experiments of Hirst and Godfrey (1993) and Schneider (1998). However, note that our model does not include a complete Indian Ocean and that the response in the Agulhas region is not simulated, hence the ampli-

Experiment	*ITF*	*Pacific 30°S*
Control	-0.92	0.25
NINO	-0.88	0.27
NINA	-0.97	0.17
NINO-ITF5	-0.48	-0.04
NINA-ITF15	-1.4	0.4

Table 2: Heat transports (PW) at sections at the ITF latitude and at 30°S in the Pacific only.

tude of the response may be unrealistic. Too much heat might transfer back into the South Pacific without being vented off to the atmosphere. On the other hand, we did not close the ITF completely, but make a more realistic change by changing the winds. The change in the OHT is completely determined by a change in the OHT_{ovt}. A complete closure as in Hirst and Godfrey (1993) almost certainly also affects the OHT_{gyre} significantly.

When changes in the winds are combined with changes in the ITF volume transport, the almost exact cancellation of OHT_{gyre} and OHT_{ovt} breaks down. The heat transport in the Northern Hemisphere is hardly affected by changes in the ITF, but the Southern Hemisphere heat transports respond strongly (Fig. 8c,d). The response of OHT_{gyre} is very similar as in experiments NINO and NINA; it is the OHT_{ovt} that responds differently. The changes in heat transport due to tropical wind variability and variability in ITF transport are almost linearly additive.

The SST difference between NINO-ITF5 and NINA-ITF15 is shown in Figure 9b. Many aspects of this change compare well with the decadal SST changes found by Zhang et al. (1997), such as warming in the central tropical Pacific, cooling in the midlatitudes. Including the changes in ITF diminished the cooling in the eastern Pacific in the NINO-ITF5 case to almost zero. Cooling in the midlatitudes is stronger than without ITF transport changes. These aspects make the differences between NINO-ITF5 and NINA-ITF15 more characteristic of decadal ENSO-like variability than the differences between NINO and NINA alone.

3.4 Response to extratropical anomalous wind forcing

Finally, we study how anomalous atmospheric forcing in the extratropics can affect tropical ocean heat transport. In the midlatitudes water subducts and flows subsurface towards the equator where it upwells again. Anomalous atmospheric forcing in the extratropics can potentially influence the tropical stratification. Model studies indicate that this mechanism does not produce anomalies of significant amplitude on decadal time scales (Schneider et al. 2000; Hazeleger et al. 2001b). However, on longer time scales the tropical thermocline can be influenced by the extratropical forcing anomalies. Hazeleger et al. (2001a) found that

cooling of about 40 W m^{-2} by transient eddy fluxes in the atmosphere in the extratropics can cool the tropical thermocline by as much as 1 Kelvin.

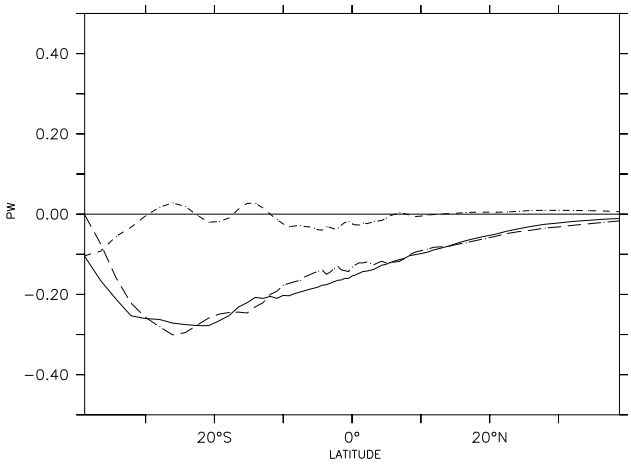

Figure 10: Difference in heat transport in SPD1 and SPD2 (in PW=10^{15}W). Continuous line: total transport; long dashed: overturning heat transport (OHT_{ovt}); short dashed: gyre heat transport (OHT_{gyre}).

Here we applied a typical atmospheric forcing anomaly to the model in the South Pacific (Fig. 2b). The response of the OHT is an increase in poleward heat transport in experiment SPD1 compared to experiment SPD2 (see Fig. 10). Strengthening of the westerlies in the southern midlatitudes east of the dateline induces a cooling (see Fig. 12a). The westerlies decrease west of the dateline and the SST warms. This is due to changes in surface heat loss induced by the wind variations. The subsurface response is rather different. The cooler waters in the eastern midlatitudes subduct and spread westward subsurface along 15°S (Fig. 12b). This cooling in the east sets up an anomalous overturning circulation that reaches into the tropics and even into the North Pacific (Fig. 11). The changes in the total heat transport within the tropics are as big as in the NINO/NINA experiments. The anomalous overturning does not consist of a change in the wind-driven Subtropical Cell. In this case, it is a deeper reaching buoyancy-driven overturning circulation. Its downwelling branch is located at the region of maximal cooling, which is much further south than the downwelling branch of the Subtropical Cell that is related to Ekman pumping. The strength of this anomalous overturning is proportional to the meridional density gradient and the vertical diffusivity in the interior of the ocean (e.g. Gnanadesikan 1999). The anomalous warm waters in the western midlatitudes spreads out subsurface to the east. The warming in the midlatitudes and cooling in the subtropics is consistent with the convergence of ocean heat transport poleward of 30°S and divergence equatorward of 30°S.

The lack of a contribution of OHT_{gyre} is due to the small zonal deviations in the temperature anomalies that are generated. While the SST cools in the east and warms in the west,

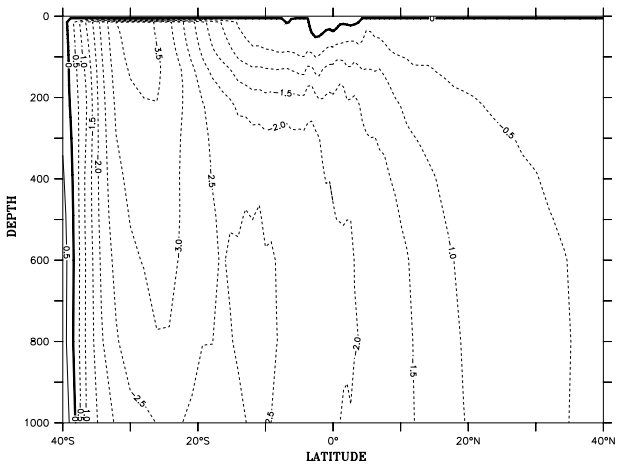

Figure 11: Difference in meridional overturning in SPD1 and SPD2 (in Sv).

the vertically integrated temperature has hardly any zonal variation (Fig. 12b). The horizontal barotropic transport enhances with 18 Sv, but due to the small temperature variations this hardly affects OHT_{gyre}.

The influence of the midlatitudes on the tropics complicates the idealized picture of heat transport by coupled overturning circulations in the atmosphere and ocean. Tropical heat transport is driven by a buoyancy-driven overturning cell that extends into the mid-latitudes, as well as by a low latitude wind-driven overturning. Since the buoyancy-driven influences do not change tropical SST (see Figure 12), presumably the tropical atmospheric circulation -including heat transport- is unchanged.

4 Discussion and conclusions

The mechanisms and sensitivity of heat transport in the tropical Pacific has been investigated in this paper. This was motivated by questions of how the total heat transport is partitioned between the atmosphere and ocean. Observations indicate that large changes in the heat transport have occured in the last decade (e.g. McPhaden and Zhang 2002). Held (2001) has presented an idealized model of the tropics that gets the proportionality correct and suggests that it is hard to change. Held assumed that the OHT was dominated by the Ekman-driven mean meridional overturning. Here, we have shown that the gyre transport cannot be ignored since it moves as much heat equatorward as the Ekman overturning moves northward. Further we have shown that the wind-driven mean meridional overturning only accounts for half of the total overturning transport in the model. The remainder must be buoyancy-driven, partly due to strong mixing near the equator. These results suggest the heat transport and the partitioning between atmospheric and oceanic heat transport may

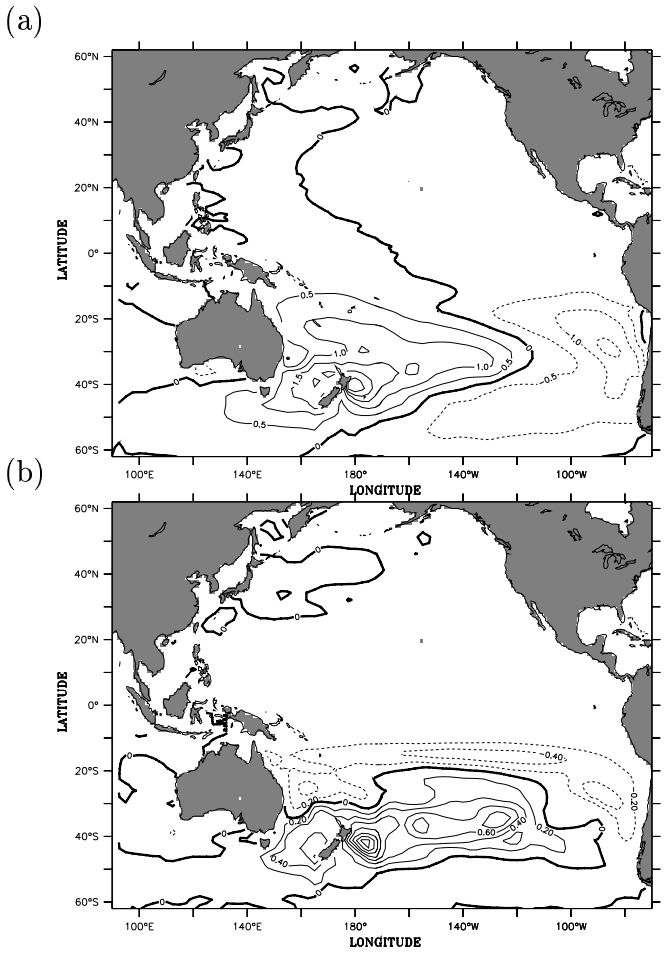

Figure 12: (a) Difference between SST (degrees C) in experiment SPD1 and experiment SPD2. (b) Difference between temperature averaged over the top 1000 m (degrees C) in experiment SPD1 and SPD2.

be more variable than Held suggests.

4.1 Summary of model results

Here we focussed only on the oceanic side of the problem. By applying El Niño-like wind anomalies, we studied the effect of long term El Niño-like variability on the heat transport. We study the stationary response of ocean heat transport to atmospheric forcing. The response of the model bears resemblance to decadal variations found in observations. The SST response consists of a strong warming in the center of the tropical Pacific, hardly any change in the cold tongue, and cooling in the midlatitudes. The pattern differs from the transient response of the ocean during the interannual El Niño cycle. In that case, the cold tongue is strongly affected. Zhang et al. (1997) did find cold tongue transitions at low frequencies, but the response in the cold tongue depends on the period of analysis.

The response of the heat transport to the large El Niño-like changes is relatively small, but significant (0.05 PW compared to the Control experiment). Large changes in the circulation occur that impact the overturning and the gyre circulation. The El Niño-like winds imply relaxing of the trades and reduced Ekman-driven overturning transport, hence reduced overturning heat transport by as much as 0.2 PW. However, the Sverdrup response of the gyres implies a slow down of the horizontal circulation. This causes equatorward heat transport by the horizontal flow to reduce, thereby compensating the reduction in poleward overturning heat transport. In our model the changes in the overturning heat transport are larger, such that persistent El Niño-like forcing induces a reduction in poleward heat transport.

The tropical Pacific is not a closed system, and the picture gets complicated by transport of heat to other regions. The ITF transports large amounts of heat into the Indian Ocean consistent with earlier model studies. Our results showed that reduced ITF transport, as observed during ENSO, cools the Indian Ocean and warms the South Pacific Ocean. The ocean heat transport only responds in the Southern Hemisphere. Increased ITF transport increases the poleward heat transport in the Indian Ocean and decreases it in the South Pacific (0.2 PW reduction) which therefore cools. In the equatorial Pacific the reduced ITF and El Niño-like winds cause the poleward heat transport to reduce by about 0.1 PW.

Finally, extratropics-tropics interaction can also influence tropical ocean heat transport in our model. Changes in extratropical atmospheric circulation can excite a buoyancy-driven overturning that reaches into the tropics, but leaves tropical SST unchanged. Cooling in the extratropics increases the poleward oceanic heat transport by 0.1 PW in the tropics.

In conclusion, tropical heat transport is rather insensitive to tropical atmospheric variability as the overturning heat transport and the gyre heat transports tend to compensate. Changes in the ITF and buoyancy forcing in the extratropics have a larger impact on tropical ocean heat transport. Increased ITF transport will reduce poleward heat transport in the South Pacific, while cooling in the midlatitudes tends to enhance poleward heat transport in the tropics. These findings were obtained in a model that ignores the dynamical response of the atmosphere to variations in ocean heat transport. Nevertheless, it is clear that the idealized model for meridional heat transport in the tropics as envisaged by Held (2001) is invalid. The most important conclusion is that the oceanic heat transports are not tightly constrained to the atmospheric heat transport due to the large heat transport by the horizontal gyre flow. The compensating effect of overturning and gyre heat transport in the tropics is a robust effect which can be understood from the response of the wind-driven circulation to atmospheric variability. However, the picture gets complicated by external sources and sinks of heat, such as the ITF and heat transport to and from the midlatitudes.

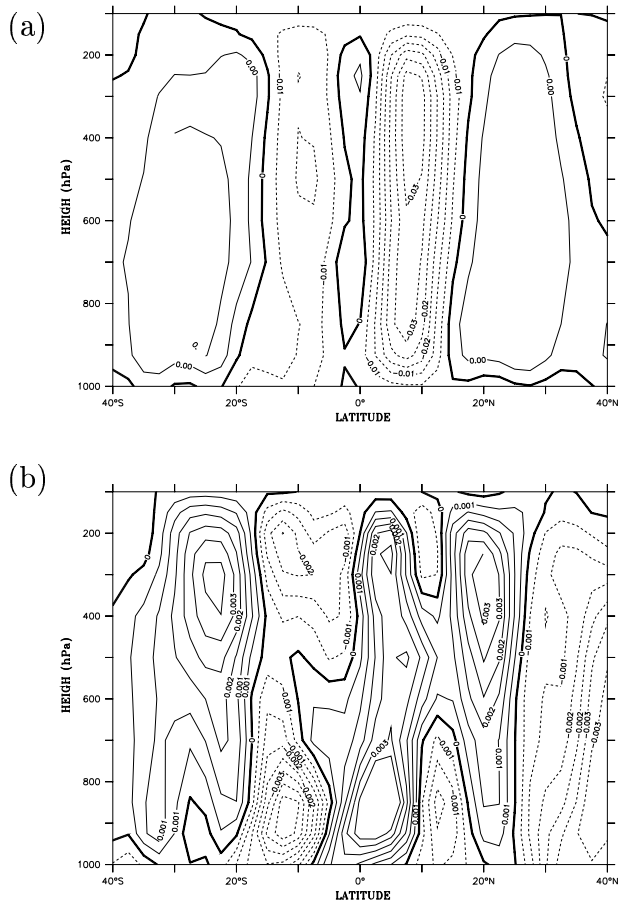

Figure 13: (a) Zonal mean pressure vertical velocity (Pa s^{-1}) in the Pacific (130°E, 70°W) averaged from 1985-2000 as obtained from NCEP/Reanalysis data (Kalnay et al. 1996). (b) Difference between zonal mean pressure vertical velocity in the Pacific (1993-2000 minus 1985-1992) .

4.2 Relation to observed decadal changes in the tropical Pacific

Observations show that the oceanic overturning mass transport has reduced steadily from the mid 1970s to the late 1990s (McPhaden and Zhang 2002). Over this period the SST in the equatorial Pacific has increased and the winds have become more akin to a typical El Niño pattern with weaker trade winds. McPhaden and Zhang suggested that decreased meridional overturning caused a reduction in poleward heat transport that caused the equatorial warming with the changes in SST being damped by surface fluxes. Our results indicate that it is premature to deduce changes in the total ocean heat transport from changes in the overturning alone because we also expect that reduced trade winds would reduce the equatorward heat transport by the gyres and also reduce the ITF, although the latter would add to the changes in overturning heat transport in the South Pacific. The changes in total

poleward ocean heat transport from the mid 1970s to the late 1990s is the sum of these different process and is unknown.

The reduced ocean overturning from the mid 1980s to the late 1990s is consistent with reduced meridional overturning in the atmosphere over the Pacific Ocean over the same time period (Fig. 13). However a reduced Pacific sector Hadley Cell need not mean reduced poleward heat transport in the atmosphere. The warming of the equatorial Pacific and the cooling in the subtropics causes the moist static energy gradient to change; hence advection of moist static energy by the mean overturning can compensate the reduced transport of mean moist static energy by the reduced overturning.

Wielicki et al. (2002) report that over the mid 1980s to late 1990s period the net incoming radiation at the top of the atmosphere over the tropics between 20°N and 20°S reduced by about 4 Wm^{-2}. The changes in ocean heat transport suggested by McPhaden and Zhang (2002), and the reduced Pacific sector Hadley Cell shown in Fig. 13, only move heat within the tropics. The net radiative loss in the tropics indicated by Wielicki et al. needs to be balanced by either reduced heat export from the tropical atmosphere or ocean to higher latitudes or by reduced heat storage in the tropical ocean. A 4 Wm^{-2} reduction in net incoming radiation over 20°S to 20°N requires a 0.5 PW reduction in the sum of the poleward heat transports across the northern and southern boundaries. Our results show that this represents a very large (about 50%) change in the ocean heat transport, and none of our experiments lead to changes in the heat transport by anywhere near that much. It is a much smaller fractional change of the atmospheric heat transport. The large tropical ocean warming over this time period makes reduction of ocean heat storage an unlikely balancing mechanism. More work is required to clarify the physical mechanisms that underlie such changes in the regional radiative balance of the climate system and apparent changes in partitioning of the total heat transport between the atmosphere and ocean.

Acknowledgements. WH thanks the people at LDEO for their hospitality during his stay. Martin Visbeck is thanked for discussions and suggestions on the topic. RS, MAC, and NN were supported by NOAA grants UCSIO PO 10196097 and NA16GP2024 and NSF grant ATM-9986515.

Appendix 1. Idealized models of ocean heat transport

a) an idealized model of heat transport by the Subtropical Cell.

The heat transport in the wind-driven Subtropical Cell can be estimated from the surface conditions only. We assume that the poleward upper branch of the Subtropical Cell is in the upper layer and the equatorward return flow in the interior. In this case, the ocean heat transport in the surface layer can be estimated using (all zonal integrals are omitted

for clarity):

$$OHT_s(y) = \rho_w c_p v_s(y) H T_s(y) \tag{3}$$

With ρ_w is the density of water, c_p the heat capacity of water, v_s the merdional surface velocity, H the thickness of the upper layer and T_s the sea surface temperature, and y is the latitude. For simplicity latitudinal and longitudal dependencies of x and y are omitted here.

The ocean heat transport in the return flow in the interior is equal to:

$$OHT_i(y) = \rho_w c_p \int_H^Z v_i(y) T_i(y) dz \tag{4}$$

Using mass conservation and the assumption that diapycnal transports are zero in the interior (this approach is similar to Klinger and Marotzke 2000), the equatorward meridional mass and heat transport at a section in the interior should balance the total mass and heat transport that is pumped down northward of the section:

$$OHT_i(y) = \rho_w c_p \int_H^Z v_i(y) T_i(y) dz = \rho_w c_p \int_{y_n}^y w(y') T_s(y') dy' \tag{5}$$

From mass conservation $w(y') = -H \partial v_s(y')/\partial y$. Integrating by parts leads to the following relation for the total surface and interior ocean heat transport:

$$OHT(y) = \rho_w c_p v_s(y_n) T(y_n) H - \rho_w c_p H \int_{y_n}^y v_s \frac{\partial T_s}{\partial y'} dy' \tag{6}$$

Here y_n is the northern boundary of the Subtropical Cell. The surface velocity v_s can be derived from the Ekman transport. Here we will use a frictional Ekman balance, such that the transport near the equator can be included:

$$v_s = \frac{1}{\rho_w (f^2 + r^2)} (r\tau_y - f\tau_x) \tag{7}$$

With f is the Coriolis parameter, r a linear friction parameter (order of days) and τ_x, τ_y are the zonal and meridional wind stress.

b) an idealized model of heat transport by the gyres.

Using the Sverdrup balance an estimate can be obtained of the heat transport by the horizontal gyres. We assume that the transport in the western boundary currents compensate the transport in the interior (i.e. away from the western boundary currents, sucht that the heat transport by the gyres is:

$$OHT_{gyre} = D \rho_w c_p [T_b \int_{x_w}^{x_{wb}} v_b dx + \int_{x_{wb}}^{x_e} v_{int} T_{int} dx] \tag{8}$$

Here D is the depth, T_b is the temperature in the western boundary current, T_{int} is the temperature away from the western boundary, x_e is the longitude of the eastern boundary, x_w is the longitude of the western boundary, x_{wb} is the latitude of the eastern edge of the western boundary current. And using the Sverdrup balance the heat transport by the gyres is (with $\beta = df/dy$):

$$OHT_{gyre} = \frac{c_p}{\beta}\frac{\partial \tau_x}{\partial y}(T_{int} - T_b)(x_e - x_{wb}) \tag{9}$$

5 References

Bishop, J.K.B., and Rossow, W.B., 1991: Spatial and temporal variability of global surface solar irradiance. *J. Geophys. Res.*, **96**, 16839-16858.

Bryan, K., 1982: Seasonal variation in meridional overturning and poleward heat transport in the Atlantic and Pacfic Oceans: a model study. *J. Mar. Res.*, **40**, supplement, 39-53, 1982.

Bjerknes, J., 1964: Atlantic air/sea interaction. *Adv. Geophys.*, **10**, 1-82.

Da Silva, A.M., C.C. Young, and S. Levitus, *Atlas of surface marine data 1994*, vol 1, *Algorithms and Procedures, NOAA Atlas 6*, 83 pp. Natl. Oceanic and Atmos. Admin., U.S. Dep. of Commer., Washington, D.C., 1994.

Fieux, M., R. Molcard, and A.G. Ilahude, 1996: Geostrophic transport of the Pacific-Indian Oceans Throughflow. *J. Geoph. Res.*, **101**, 12421-12432.

Ganachaud, A., and C. Wunsch, 2000: Improved estimates of global ocean circulation, heat transport and mixing from hydrographic data. *Nature*, 453-457.

Ganachaud, A., and C. Wunsch, 2002: Large-scale ocean heat and freshwater transports-during the World Ocean Circulation Experiment. *J. Climate in press.*

Gnanadesikan, A., 1999: A simple predictive model for the structure of the oceanic pycnocline. *Science*, **283**, 2077-2079.

Gordon, C. et al., 2000: The simulation of SST, sea ice extents and ocean heat transports in a version of the Hadley Centre coupled model without flux adjustments. *Clim. Dyn.*, **16**, 147-168.

Guilderson, T.P., and D.P. Schrag, 1998; Abrupt shift in subsurface temperatures in the tropical Pacific associated with changes in El Niño. *Science*, **281**, 240-243.

Hazeleger. W., R. Seager, M. Visbeck, N. Naik, and K. Rodgers, 2001: Impact of midlatitude storm track on the upper Pacific Ocean. *J. Phys. Oceanogr.*, **31**, 616-636.

Hazeleger, W., M. Visbeck, M. Cane, A. Karspeck, and N. Naik, 2001: Decadal upper ocean variability in the tropical Pacific. *J. Geoph. Res.*, 106, 8971-8988.

Held, I.M., 2001: The partitioning of the poleward energy transport between the tropical ocean and atmosphere. *J. Atmos. Sc.*, **58**, 943-948.

Hirst, A.C., and J.S. Godfrey, 1993: The role of the Indonesian Throughflow in a global GCM. *J. Phys. Oceanogr.*, **23**, 1057-1086.

Jayne, S.R., and J. Marotzke, 2001: The dynamics of ocean heat transport variability. *Rev. Geophys.*, **39**, 385-411.

Kalnay, E. et al., 1996: The NCEP/NCAR 40-year reanalysis project. *Bull. Am. Meteorol. Soc.,* **77**, 437-471.

Klinger, B.A., and J. Marotzke, 2000: Meridional heat transport by the subtropical cell. *J. Phys. Oceanogr.*, **30**, 696-705.

Levitus, S. and T.P. Boyer, 1994: World Ocean Atlas 1994, volume 4: Temperature, *NOAA ATLAS NESDIS 4.*

Levitus, S., R. Burgett, and T.P. Boyer, 1994: World Ocean Atlas 1994, volume 3: Salinity, *NOAA ATLAS NESDIS 3.*

McPhaden, M.J., and D. Zhang, 2002: Slowdown of the meridional overturning circulation in the upper Pacific Ocean. *Nature*, **415**, 603-608.

Meyers, G., 1996: Variation of the Indonesian Throughflow and the El Niño Southern Oscillation. *J. Geoph. Res.*, **101**, 12255-12263.

Pedlosky, J., 1996: Ocean circulation theory. *Springer-Verlag*, Berlin Heidelberg, 453pp.

Schneider, N., 1998: The Indionesian Throughflow and the global climate system. *J. Climate*, **11**, 676-689.

Seager, R., M.B. Blumenthal, and Y. Kushnir, 1995: An advective atmospheric mixed layer model for ocean modeling purposes: Global simulation of surface heat fluxes. *J. Climate*, **8**, 1951-1964.

Seager, R., Y. Kushnir, N.H. Naik, M.A. Cane, J. Miller, 2001: Wind-driven shifts in the latitude of the Kuroshio-Oyashio extension and generation of SST anomalies on decadal timescales. *J. Climate*, **14**, 4249-4265.

Semtner, A.J., and R.M. Chervin, 1992: Ocean general circulation from a global eddy resolving model. *J. Geophys. Res.*, **97**, 5493-5550.

Timmermann, A., M. Latif, A. Bacher, J. Oberhuber, E. Roeckner, 1999: Increased El Niño frequency in a climate model forced by future greenhouse warming. *Nature*, **398**, 694-696.

Toggweiler, J., K. Dixon, and W. Broecker, 1991: The Peru upwelling and the ventilaion of the South Pacific thermocline. *J. Geoph. Res.*, **96**, 20467-20497.

Trenberth, K.E., and J.M. Caron, 2001: Estimates of meridional atmosphere and ocean heat transports. *J. Climate*, bf 14, 3433-3443.

Visbeck, M., H. Cullen, G. Krahmann, and N. Naik, 1998: An ocean's model response to north atlantic oscillation-like wind forcing. *Geophys. Res. Letters*, **25**, 4521–4524.

Vranes, K., A.L. Gordon, and A. Ffield, 2002: The heat transport of the Indonesian Throughflow and implications for the Indian Ocean heat budget. *Deep Sea Res. II*, 1391-1410.

Wielicki, B.A., et al., 2002: Evidence for large decadal variability in the tropical mean radiative energy budget. *Science*, **295**, 841-844.

Zhang, Y., J. M. Wallace, and D. S. Battisti, 1997: ENSO-like interdecadal variability: 1900-1993, *J. Climate, 10,* 1004-1020.